

Intramolecular Hydrogen Bonding in Disubstituted Ethanes: General Considerations and Methodology in Quantum Mechanical Calculations of the Conformational Equilibria of Succinamate Monoanion

Mark S. Rudner, David R. Kent, IV, William A. Goddard, III, and John D. Roberts*

Chemical Laboratories and Beckman Institute, California Institute of Technology, Pasadena, California 91125

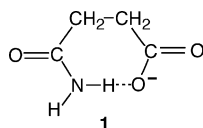
Received: June 2, 2005

The importance of intramolecular hydrogen bonding between the carboxylate oxygen and amide proton of succinamate anion has been investigated by quantum mechanical simulations as a function of solvent for comparison with conformational equilibria estimated by NMR spectroscopy. The focus is on those methodological considerations of general interest to the conformational equilibrium problem, which are also particularly relevant to the quantum calculations. The roughly planar symmetry of the amide and carboxylate substituents of succinamate anion and the possibility of intramolecular hydrogen-bond formation together suggest that the orientational degrees of freedom of the substituents could play an important role in the equilibrium of the CH₂–CH₂ torsion. To test this hypothesis, two-dimensional potential-energy surfaces (PESs) were mapped out from the quantum mechanical calculations, with coordinates corresponding to the CH₂–CH₂ torsional and amide group rotational degrees of freedom. The Boltzmann populations obtained from two-dimensional PESs and those obtained from a one-dimensional adiabatic surface for the CH₂–CH₂ torsion were compared with the experimental results. In these comparisons, the agreement of calculated gauche fractions with corresponding experimental values was checked, as well as the agreement between predicted coupling constants and those determined from experimental spectra. In polar protic and aprotic solvents, where highly polar trans conformations can be stabilized by dipole–dipole and hydrogen-bonding interactions with the solvent, the orientational degree of freedom of the amide substituent appears to play a sufficiently important role in the CH₂–CH₂ torsional equilibrium that it cannot be safely ignored in the simulations.

Introduction

We are interested in the effects of hydrogen bonding on the conformational preferences of small molecules that have the ability to form internal (and external) hydrogen bonds. While one might expect that intramolecularly hydrogen-bonded conformations would dominate all others in the conformational mix, there are important competing factors that can decrease the importance of hydrogen bonding in the conformational equilibrium. First, internal hydrogen bonding may only be possible from a very restricted set of conformations which may otherwise be energetically less favorable than the majority of the non-hydrogen-bonded conformations. This leads to an entropic penalty for hydrogen bonding. Additionally, interactions with the solvent including external hydrogen-bond formation can compete directly with the internal hydrogen-bond interactions to favor more open conformations.^{1,2}

We have studied these effects through the conformational analysis of the possible role of carboxylate to amide hydrogen succinamate monoanion (**1**) using nuclear magnetic resonance (NMR) experiments and quantum mechanical simulations.³ The experiments involved a wide range of protic, aprotic, and nonpolar solvents. Simulations reported here were performed at a different level than previously and focused on three solvents of rather different character, namely water, acetone, and dioxane.



Anion **1** presents an interesting test platform for several reasons. First, it is possible for one of its amide protons to form an intramolecular hydrogen bond with one of its negatively charged carboxylate oxygens. Second, the experimental results³ and quantum mechanical simulations indicate that, at least in some solvents, the conformer populations are near the pure statistical values of 2:1. In this regime, the predicted conformer distributions are most sensitive to changes in the calculated relative energies of the conformers. At room temperature, $k_B T = 0.59$ kcal/mol; this sets the relevant energy scale by which changes in computational results must be compared and indicates that the theoretical calculations of *relative* energies need to be accurate to within 0.1–1 kcal/mol to achieve even qualitative agreement with experimental results. While this makes it even more difficult to achieve good agreement between experiment and theory, this sensitivity forces us to find ways of refining our methods to capture more than just the simplest effects. As part of this refinement, because of the planar shape of carboxylate groups and the possibility of intramolecular hydrogen-bond formation, it was necessary to investigate whether the substituent-orientational degrees of freedom could exert an important influence on the conformational equilibria of the CH₂–CH₂ torsion and consequently influence the observed vicinal proton–proton couplings.

Quantum Mechanical Calculations

All quantum mechanical calculations were made with Jaguar version 4.2 release 77 (Schrodinger, Inc.) using Becke 3-LYP type density functional theory (DFT).⁴ To investigate the effect

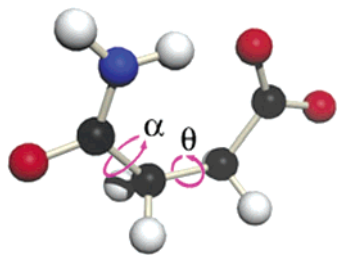


Figure 1. Definition of the angles manipulated in the quantum mechanical calculations.

of basis set on the calculations and to ensure the convergence of all final results, the following series of basis sets was employed in the calculations: 6-31G**, 6-31G**+, 6-311G**+, aug-cc-pVDZ, and aug-cc-pVTZ(-f).^{5,6} The (-f) in aug-cc-pVTZ(-f) indicates that no f-type functions were used in this basis set.

Solution-phase calculations were modeled using the continuum-solvation approximation. This method finds self-consistent solutions for the Schrödinger and Poisson–Boltzmann equations describing a molecule in a cavity with $\epsilon = 1$ (vacuum) suspended in an infinite dielectric block; these solutions were found using the PS Solve package of Jaguar with solvent parameters as follows: acetone, $\epsilon = 20.7$, $R_{\text{probe}} = 2.44$ Å; dioxane, $\epsilon = 2.209$, $R_{\text{probe}} = 2.57$ Å; water, $\epsilon = 80.37$, $R_{\text{probe}} = 1.40$ Å. Although the succinate species studied is anionic, no positively charged counterions were incorporated in the calculations, because the incorporation of multiple solute cavities is not supported by the current Poisson–Boltzmann solvation model. This limitation is one of the possible sources of error in the calculations but might also be taken as representing the results of calculations at infinite dilution, at least to the extent that such conditions are interesting.

Generation of Potential-Energy Surfaces

Because of its relevance to observed NMR proton–proton couplings and its dominant role in determining the qualitative geometric features of molecular conformations, the rotational state of the central CH₂–CH₂ bond dihedral angle is central to both experimental and theoretical work on disubstituted ethanes of this sort. Many systems such as succinic acid, succinonitrile, and β -alanine have been studied previously by mapping out simple (one-dimensional) adiabatic rotational energy curves as a function of this CH₂–CH₂ torsion.^{7,8}

While adiabatic curves of this type contain useful information about the energy landscape available to the system with respect to one important degree of freedom, at finite temperatures all degrees of freedom must, in principle, be taken into account to properly calculate the conformational statistics. For succinate, we expected that the amide substituent-orientational degree of freedom would have a large effect on the equilibrium of the CH₂–CH₂ dihedral because of its influence on hydrogen-bond formation and steric interactions. Thus, we investigated the effect of including a second degree of freedom corresponding to the orientation of the amide substituent on calculated CH₂–CH₂ dihedral angle rotamer populations.

The CH₂–CH₂ dihedral and one angle defining the amide–substituent orientation were fixed to values on a two-dimensional square grid, with all remaining geometric degrees of freedom optimized for each conformer. These two angular degrees of freedom, denoted by θ and α , are shown in Figure 1. As shorthand for referring to specific conformers, we label them by the values of these two angles using the notation (θ, α) . In a compromise between computational expense and method-

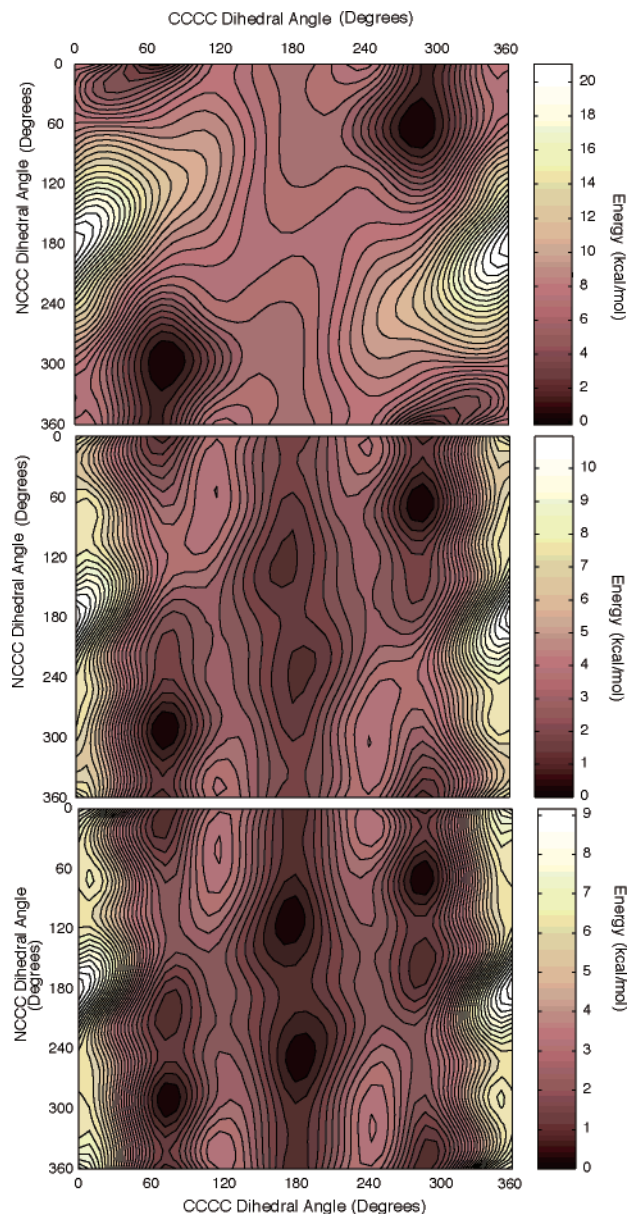


Figure 2. Theoretical PESs as a function of angles α and θ for succinate monoanion in (a) dioxane, (b) acetone, and (c) water.

ological accuracy, calculations were performed every 36° in both directions for (θ, α) on the domain $[0^\circ, 360^\circ] \times [0^\circ, 360^\circ]$. No forced symmetries were imposed on the initial structures or in the geometry optimizations. The redundancy in the grid was used to help minimize the chance of obtaining spurious results from conformers getting caught in local minima of the potential-energy surface during geometry optimization by increasing the number of nonequivalent initial (preoptimization) structures.

For plotting and statistical analysis, the PESs were fit with a two-dimensional cubic spline surface and interpolated onto a finer grid with a spacing of 9° in both directions. A Boltzmann distribution was assumed for the discrete states on the fine grid and the relative populations calculated by

$$f_{(\theta,\alpha)} = \frac{\exp(-E_{(\theta,\alpha)}/k_B T)}{\sum_{\theta,\alpha} \exp(-E_{(\theta,\alpha)}/k_B T)} \quad (1)$$

where $f_{(\theta,\alpha)}$ is the relative amount of the species with dihedral

TABLE 1: Measured Vicinal H–H Couplings and Calculated Gauche Fractions for Succinamate Monoanion in Various Solvents³

solvent	J_{13} , Hz	J_{14} , Hz	% G^a (J_{13})		% G^a (J_{14})		% G^a (avg)	
D ₂ O	6.85	8.28	59	51	57	50	58	51
ethanol	6.89	8.48	59	52	55	48	57	50
<i>t</i> -butyl alcohol	7.92	5.86	80	69	80	69	80	69
acetone	9.04	3.90	102	89	98	85	100	87
DMSO ^b	8.41	5.32	89	78	85	74	87	76
dioxane ^c	8.96	3.77	100	88	98	86	99	87
THF	9.13	3.08	103	90	105	92	104	91

^a Altona procedure calculated gauche populations for $\theta_g = 60^\circ$ (left column) and $\theta_g = 70^\circ$ (right column). ^b This succinamate sample contained 0.5 \times as much water as the succinamate anion in DMSO. ^c This succinamate sample contained 6 \times as much water as the succinamate anion in dioxane.

angles θ and α as defined earlier, $E_{(\theta,\alpha)}$ is the energy of conformer (θ , α), k_B is the Boltzmann constant, and T is the absolute temperature. The θ -rotamer populations were calculated by summing the probabilities over α for each value of θ , eq 2.

$$P_\theta = \sum_{\alpha=0^\circ}^{360^\circ} f_{(\theta,\alpha)} \quad (2)$$

For comparison, we also calculated the adiabatic populations considering only the lowest-energy structure for each value of θ

$$p_\theta^{\text{ad}} = \frac{\exp(-E_\theta^{\text{min}}/kT)}{\sum_\theta \exp(-E_\theta^{\text{min}}/kT)} \quad (3)$$

with

$$E_\theta^{\text{min}} = \min_\alpha E_{(\theta,\alpha)} \quad (4)$$

This procedure thus recreated the results of the simpler one-dimensional adiabatic model (see Figure 5).

Experimental Results

Our experimental studies of the conformational preferences of succinamic acid utilized the NMR and analytical techniques for the calculations of conformational equilibria described elsewhere.³

The theoretical calculations strongly indicated that the gauche angle should be substantially larger than 60° (see below). Thus, the results of our analyses are reported twice, once with the classical gauche angle between the substituents of 60° and once with the gauche angle set to 70° . Experimentally determined J_{13} and J_{14} coupling constants, gauche populations estimated from these coupling constants, and amide proton chemical shifts for succinamate monoanion are presented in Table 1.

Results and Analysis

Figure 2 shows the PESs for succinamate monoanion calculated with the aug-cc-pVTZ(-f) basis set in dioxane, acetone, and water solvents. To investigate the convergence of these calculations, PESs for each solvent system were generated with basis sets 6-31G**, 6-31G**+, 6-311G**+, aug-cc-pVDZ, and aug-cc-pVTZ(-f). PESs from different basis sets were then compared by forming the point-by-point difference surface (Figure 3). Visual inspection of the plots of these difference surfaces aided in the tracking of the convergence of

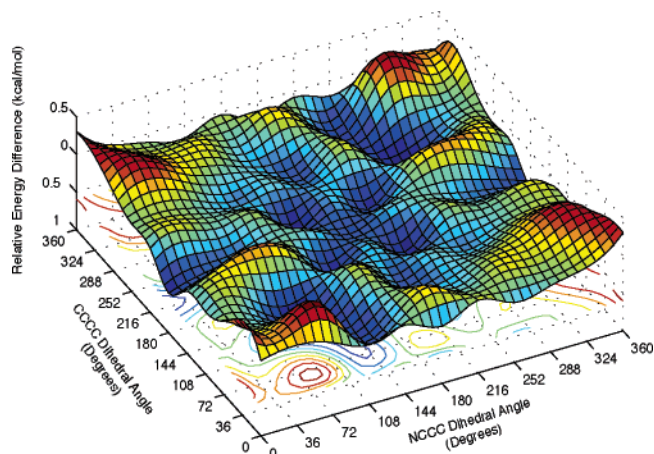


Figure 3. Sample energy-difference surface for succinamate monoanion in water, calculated by taking the point-by-point energy difference between the PESs generated using the aug-cc-pVTZ(-f) and aug-cc-pVDZ basis sets. The root-mean-squared deviation in this plot is $\sigma = 0.18$ kcal/mol. Plots of this type were used to examine the convergence of our calculations with basis set size and composition.

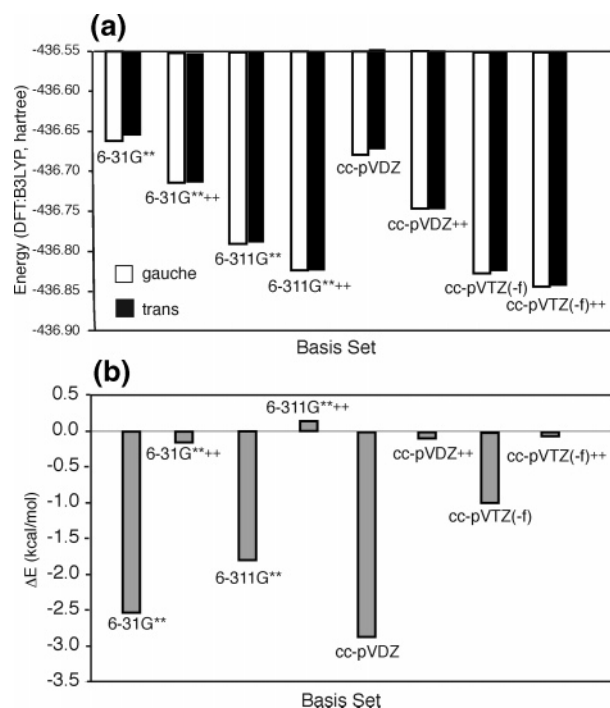


Figure 4. Convergence of quantum calculations with basis set. In (a), the absolute energy for fully optimized gauche and trans structures is plotted for each basis set. In (b), the plots are of energy differences between these fully optimized gauche and trans structures.

our calculations across changes in basis set. The standard deviations of these surfaces added a further quantitative measure of convergence.

Convergence was also monitored by plotting the absolute energy of the lowest-energy gauche and trans structures for each basis set in aqueous solvent (Figure 4a). The convergence with increasing basis set size within each family is clearly evident in this plot. Figure 4b shows the energy difference between the lowest-energy gauche and trans structures for each basis set in aqueous solution. Similar plots were made for the other solvents and are summarized in Table 2.

The relative energies of the gauche and trans conformers are very different depending on whether diffuse functions are included in the basis set. Recent work by Lynch and co-workers⁹ underscored the need for including diffuse functions in basis

TABLE 2: Summary of Convergence Data for B3LYP Calculations in Three Solvents as Measured by the Standard Deviation of the Changes in the Point-by-Point Energy Difference Surface as the Basis Set Was Changed

basis set	N_{basis}	$\sigma_{\Delta E}$, dioxane ^a kcal/mol	$\sigma_{\Delta E}$, acetone ^a kcal/mol	$\sigma_{\Delta E}$, water ^a kcal/mol
6-31G**	150			
6-31G**++	188	0.99	1.04	0.96
6-311G**++	218	0.27	0.24	0.39
aug-cc-pVDZ	238	0.26	0.21	0.33
aug-cc-pVTZ(-f)	334	0.23	0.18	0.18

^a The $\sigma_{\Delta E}$ value on line k is the standard deviation of the energy difference surface corresponding to the basis sets listed on lines k and $(k - 1)$.

sets for DFT calculations. Because the method converges to its theoretical limitations as more functions are added to a given basis set, we conclude that diffuse functions are absolutely necessary for calculations of this type. The comparison of our theoretical with experimental results³ also strongly supports this conclusion (see below).

The results of our theoretical calculations of the conformational preferences of succinamate are reported in Table 3. *Gauche* populations were calculated by summing over all conformations with θ between -120° and $+120^\circ$ with the aid of eq 3. To compare with the one-dimensional adiabatic method,

$$\% G = \sum_{\theta=-120^\circ}^{120^\circ} p_\theta \quad (3)$$

gauche populations were also calculated by summing up the populations of only the conformers of lowest energy (with respect to α) for θ between -120° and 120°

$$\% G_{\text{ad}} = \sum_{\theta_i=-120^\circ}^{120^\circ} p_{\theta_i}^{\text{ad}} \quad (4)$$

These populations are presented in the columns labeled $\% G_{\text{ad}}$ of Table 3.

The changes in these results with basis set size give further evidence for the necessity of large basis sets with diffuse functions. With the exception of water with 6-311G**++, the trend is very clear. We have no explanation for this anomalous case. For both acetone and water, where the conformational equilibrium is less than 100% *gauche*, the results are sensitive to basis set size and composition. Because $k_B T$ is approximately 0.59 kcal/mol at room temperature, a high standard of convergence is needed in order to report reliable results for the conformational populations. For these systems, it appears that *at least* a triple- ζ basis set with diffuse functions is needed. Judging by the change in going from the correlation-consistent double- ζ (aug-cc-pVDZ) to triple- ζ (aug-cc-pVTZ(-f)) basis sets, we estimate that moving up to a quadruple- ζ basis set would change the populations by less than about 5% for acetone and water, and would have no observable effect on the dioxane results.

It is both interesting and important to notice the differences between the results calculated using the full two-dimensional PESs and the one-dimensional adiabatic results. Here, the one-dimensional method tended to overestimate the *gauche* fraction in all cases by about 10–20%. Figure 5 shows the one-dimensional population curves for each system, as calculated (a) by summing over the α -coordinate of the full two-dimensional PES and (b) by using just the one-dimensional adiabatic energy curve.

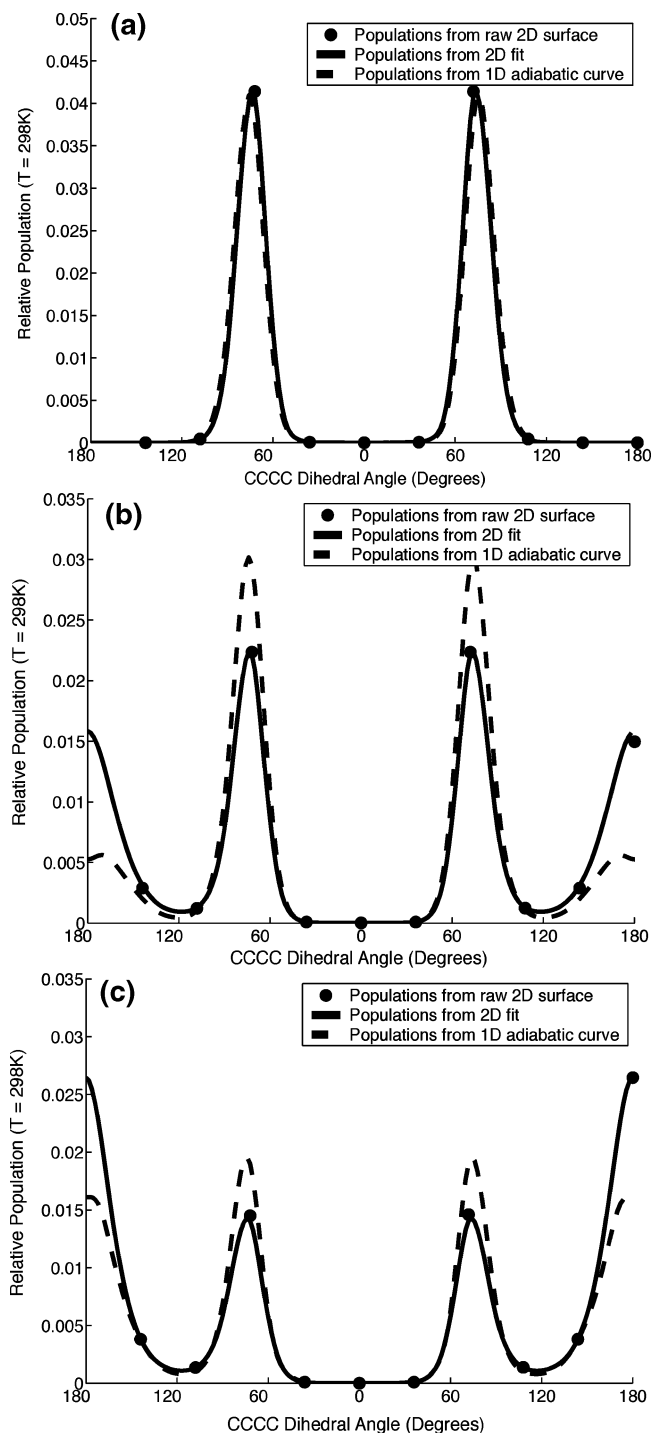


Figure 5. Boltzmann rotamer populations at $T = 298$ K from quantum adiabatic calculations using the full two-dimensional PESs and one-dimensional adiabatic energy curves for succinamate monoanion in (a) dioxane, (b) acetone, and (c) water.

Finding that consideration of the additional α degree of freedom leads to a consistent and significant change in the results is important for two reasons. First, and specific to this system, it shows that the decreased rotational freedom of the amide group in *gauche* conformations disfavors the *gauche* conformations relative to what one would expect from purely energetic considerations of representative *gauche* and *trans* conformers. This is the entropic penalty for intramolecular hydrogen-bond formation. Second, and more generally, it shows that more care must be taken in designing computational studies of this type than has historically been taken in many cases.

TABLE 3: Gauche Fractions and Mean Gauche Dihedral Angle Calculated with B3LYP Density Functional Theory as Described in the Text

basis set	N_{basis}	gauche angle θ°	% G dioxane	% G_{ad}^a dioxane	% G acetone	% G_{ad}^a acetone	% G water	% G_{ad}^a water
6-31G**	150	75	100	100	99	100	97	99
6-31G**++	188	74	100	100	51	67	45	62
6-311G**++	218	74	100	100	60	82	66	90
aug-cc-pVDZ	238	76	100	100	70	87	48	62
aug-cc-pVTZ(-f)	334	77	100	100	62	82	42	55

^a % G_{ad} values were calculated from the adiabatic one-dimensional energy curves.

Unfortunately, it is quite common in computational work employing quantum mechanical calculations for researchers to focus on only the single-point energetics of a few representative cases of a system, rather than exploring the full thermodynamic picture. Although finite computational resources do place restrictions on the amount of data that can be collected in a computational study, one must keep in mind what the limitations of any particular method are and strive to capture as much of the relevant physics in the corresponding model as possible.

Our agreement between experiment and theory is not excellent. The tendency toward trans is clearly strongest in water, but the theory predicts a larger gauche population in acetone than in dioxane, while the experiments show the reverse. Although the one-dimensional adiabatic results appear to be better than the two-dimensional results, because the gauche population values predicted by the adiabatic method for acetone and water are quite close to those estimated from the experimental coupling constants, we believe that this result is surely coincidental and that there is no real justification to accept these results as validation of the one-dimensional over the two-dimensional method.

When extracting the gauche populations from the experimental data using the modified Altona procedure¹⁰ to estimate the coupling constants for each conformation, the standard value of 60° was used for the gauche dihedral angle, as well as a value of 70° . These choices were dictated because molecular models and theoretical results indicated that the minimum of the potential energy surface was likely to be at an angle larger than 60° . The impact of this choice on some of the results begs the question of how this angle really should be chosen and calls into question the validity of this method of analyzing experimental data. The true spectrum is an average over a continuum of states corresponding to all values of θ . If the gauche and trans potential energy wells are not exceptionally deep and sharp, angles other than those of just the well bottoms will contribute significantly to the observed average couplings.

Noting the particular inherent problem in the analysis of experiments of this kind, other ways of evaluating the performance of our theoretical calculations against experimental observations were considered. The most logical approach is to compare theoretical results directly with the observed spectral features (proton–proton couplings). While the “holy grail” of this approach would be to include the electron–nuclear interactions in the quantum calculations and calculate the values of the coupling constants for each conformer on the two-dimensional potential energy surface, just calculating quantitatively accurate proton–proton couplings for a single conformer still poses a great challenge.¹¹ As a compromise, we used the dependence of J_{13} and J_{14} on θ employed by Haasnoot et al.¹² to assign values of these couplings to each angle of θ between 0° and 360° in 2° increments. Populations for each of these conformers were then calculated from our two-dimensional cubic-spline-fit PES by summing over the α -coordinate to

TABLE 4: Theoretical Coupling Constants Calculated from the Quantum Mechanical PESs and the Haasnoot Equation Relating $J_{\text{H-H}}$ to Dihedral Angle

basis set	dioxane ^a		acetone ^b		water ^c	
	J_{13} , Hz	J_{14} , Hz	J_{13} , Hz	J_{14} , Hz	J_{13} , Hz	J_{14} , Hz
6-31G**	9.9	1.8	9.7	2.0	9.6	2.2
6-31G**++	9.8	1.8	7.2	7.4	7.0	7.9
6-311G**++	9.8	1.9	7.7	6.3	8.0	5.6
cc-pVDZ++	9.7	2.0	8.2	5.3	7.1	7.7
cc-pVTZ(-f)++	9.8	1.9	7.8	6.1	6.7	8.3

^a Experimental values were $J_{13} = 8.67$ Hz and $J_{14} = 4.46$ Hz.

^b Experimental values were $J_{13} = 9.04$ Hz and $J_{14} = 3.90$ Hz.

^c Experimental values were $J_{13} = 6.85$ Hz and $J_{14} = 8.28$ Hz.

produce theoretical values for the observed statistically averaged proton–proton couplings. These results are presented in Table 4.

For water with the largest basis set, aug-cc-pVTZ(-f), the agreement looks very good. Note, however, the high sensitivity of the predicted coupling constants to basis set (and hence PES). Because no calculations were run with an even larger quadruple- ζ basis set, it is not clear exactly how much more these values could change. As estimated above, the gauche fractions should not change by more than about 5% if the basis is increased further, which should keep the coupling constants in the vicinity of 6.5–7.0 Hz and 8.0–8.5 Hz.

The situation with acetone and dioxane is not so satisfactory, because now theory and experiment disagree strongly about the conformational preferences. The fact that the acetone results disagree with the experimental results, both in terms of calculated gauche populations and in terms of predicted coupling constants, shows that there is ample room for improvement in the theory. The most likely source of this problem is the continuum-solvation model, which neglects the detailed characteristics of solvent molecules such as acetone with its locally polarizable carbonyl bond. Although this can be expected to be an equally serious problem for water, the recommended Jaguar parameters for water have been specially optimized to improve the results of calculations in aqueous solutions. This could explain the apparent better performance of the water calculations as compared to calculations in the other two solvents. Newer software versions with hand-selected parameters for other solvents such as acetone may lead to better agreement with experiment.

With regard to the trend with increasing basis set size, it is highly unlikely that a change in basis set could result in any significant improvement for the dioxane or acetone calculations. It is possible that a different flavor of DFT, or possibly higher-level ab initio calculations such as those employing MP2 corrections to the wave functions, could result in improved results using the current continuum-solvation model, but this would have to be tested in future work.

Conclusions

We present recent findings about methodology in conformational analysis in the context of a quantum mechanical study of succinamate monoanion in solutions of acetone, dioxane, and water. Several important lessons were learned with regard to this specific system, which surely apply to conformational analysis in general.

First, it was found, in accordance with the recent report of Lynch et al., that the convergence of DFT calculations requires large basis sets with diffuse functions. In water, there was an unexplained disagreement between the results from the 6-311G**++ and aug-cc-pVTZ(-f) triple- ζ basis sets. To understand the convergence requirements for this type of study, further work should be done with even larger basis sets to determine if and when the results have stabilized. Currently, however, such calculations are prohibitively computationally expensive.

The most significant result was that taking into account a second degree of freedom corresponding to the orientation of the amide substituent in our PES calculations led to important changes in the conformational equilibrium. In this case, the effect could be attributed to the fact that this second degree of freedom is much more restricted in gauche-like conformations than in trans-like conformations, thus giving the trans conformations an entropic advantage and reducing the effect of intramolecular hydrogen bonding on the conformational equilibria. More generally, however, this underscores the need to consider more than just the simplest degree of freedom in studies of this kind. When the energy profiles of any other degrees of freedom are significantly affected by rotations of the primary dihedral, then all such degrees of freedom should be considered in the calculations. Furthermore, these considerations apply to a much broader range of computational problems, where one must not neglect the importance of entropic contributions to the free energy, which could well be missed in a study consisting merely of a limited set of single-point energies.

In this work, we have studied only two degrees of freedom, but future work might consider an additional degree of freedom corresponding to rotations of the carboxylate group. However, because the computational expense grows exponentially with the number of degrees of freedom, another direction for further

work should be to look into the possibility of applying adaptive/multiscale grids to more efficiently map out the multidimensional PESs available to this kind of system.

Acknowledgment. Acknowledgment is made to the donors of the Petroleum Research Fund administered by the American Chemical Society, for support of this research. We are also deeply indebted to the National Science Foundation under grant CHE-0104273, the Summer Undergraduate Research Fellowship Program (SURF) at the California Institute of Technology, the Camille and Henry Dreyfus Foundation, Merck and Company, the E. I. Du Pont Company, and Dr. & Mrs. Chester M. McCloskey for their helpful financial assistance. D.R.K. is grateful for support of this research from a graduate fellowship from the Fannie and John Hertz Foundation. The computational resources at the MSC were provided by ARO-DURIP and ONR-DURIP. Other support for the MSC came from DOE, ONR, NSF, NIH, Chevron-Texaco, Nissan, Aventis, Berlex, Intel, and Beckman Institute.

References and Notes

- (1) Lit, E. S.; Mallon, F. K.; Tsai, H. Y.; Roberts, J. D. *J. Am. Chem. Soc.* **1993**, *115*, 9563–9567.
- (2) Price, D. J.; Jorgenson, W. L.; Roberts, J. D. *J. Am. Chem. Soc.* **1998**, *120*, 9672–9679.
- (3) Rudner, M. S.; Jeremic, S.; Petterson, K. A.; Kent, D. R. IV; Brown, K. A.; Goddard, W. A., III; Roberts, J. D. *J. Phys. Chem. A* **2005**, *109*, 9076–9082.
- (4) Becke, A. D. *J. Chem. Phys.* **1993**, *98*, 5648.
- (5) Hehre, W. J.; Ditchfield, R.; Pople, J. A. *J. Chem. Phys.* **1972**, *56*, 4233.
- (6) Hariharan, P. C.; Pople, J. A. *Theor. Chim. Acta* **1993**, *28*, 213.
- (7) Gregoire, F.; Wei, S. H.; Streed, E. W.; Brameld, K. A.; Fort, D.; Hanely, L. J.; Walls, J. D.; Goddard, W. A.; Roberts, J. D. *J. Am. Chem. Soc.* **1998**, *120*, 7337–7343.
- (8) Kent, D. R., IV; Petterson, K. A.; Gregoire, F.; Snyder-Frey, E.; Hanely, L. J.; Muller, R. P.; Goddard, W. A.; Roberts, J. D. *J. Am. Chem. Soc.* **2003**, *124*, 4481–4486.
- (9) Lynch, B. J.; Zhao, Y.; Truhlar, D. G. *J. Phys. Chem. A* **2003**, *107*, 1384–1388.
- (10) Altona, C.; Francke, R.; de Haan, R.; Ippel, J. H.; Daalmans, G. J.; Hoekzema, A. J.; Wijk, v. *Magn. Reson. Chem.* **1994**, *32*, 670–678.
- (11) Helgaker, T.; Jaszunski, M.; Ruud, K. *Chem. Rev.* **1999**, *99*, 293–352.
- (12) Haasnoot, C. A. G.; Deleeuw, F. A. A. M.; Altona, C. *Tetrahedron* **1980**, *36*, 2783–2792.